

Critical Phenomena of Contact near Phase Transitions

Y.-Y. Chen,¹ Y.-Z. Jiang,¹ X.-W. Guan,^{1,2,*} and Qi Zhou^{3,†}

¹*State Key Laboratory of Magnetic Resonance and Atomic and Molecular Physics, Wuhan Institute of Physics and Mathematics, Chinese Academy of Sciences, Wuhan 430071, China*

²*Department of Theoretical Physics, Research School of Physics and Engineering, Australian National University, Canberra ACT 0200, Australia*

³*Department of Physics, The Chinese University of Hong Kong, Shatin, New Territories, HK*

(Dated: September 29, 2022)

Contact, which measures the two-body correlations at short distances in dilute systems, is a central quantity to rule ultra cold atoms. It builds up universal relations among thermodynamic quantities, such as the large momentum tail, energy, and dynamic structure factor, through the renowned Tan relations. However, a conceptual question remains open as to whether or not Contact signifies phase transitions, which are insensitive to short-range physics. Here we show that, near a continuous classical or quantum phase transition, Contact exhibits a variety of critical phenomena, including scaling laws and critical exponents that are uniquely determined by the universality class of the phase transition, and a constant Contact per particle. We also use a prototypical exactly solvable model to demonstrate these critical phenomena in one-dimensional strongly interacting fermions. Our work establishes an intrinsic connection between the universality of dilute many-body systems and the universal critical phenomena near a phase transition.

Contact \mathcal{C} strikingly captures the universality of ultra cold atoms. As revealed by Tan relations [1–3] and their expressions in other forms[4–7], regardless of the choices of microscopic parameters, a wide range of quantities in dilute systems are governed by \mathcal{C} , which characterizes the probability of having two particles within a short distance \mathbf{d} . For instance, When \mathbf{d} approaches zero, the two-body correlation function in three dimensions follows $\int_{|\mathbf{x}-\mathbf{x}'|<d} d\mathbf{x}' \langle \hat{n}(\mathbf{x}) \hat{n}(\mathbf{x}') \rangle \sim \mathcal{C} |\mathbf{d}| / (4\pi)$, where $\hat{n}(\mathbf{x})$ is the density operator at position \mathbf{x} . Whereas the definition of Contact is apparently independent on what many-body phase the system has, there have been extensive interests to explore the behavior of Contact near a phase transition[8–17]. The success of these efforts will significantly deepen our understandings of the connection between short-ranged two-body correlations and phase transitions, which are generally believed to be disentangled with each other, since the latter one is insensitive to details of short-range physics.

Experimental studies have shown that whereas Contact of strongly interacting fermions remains finite in both the normal and the superfluid phase, evidences indicate that it gets enhanced near the superfluid transition temperature. However, due to the lack of enough resolution, it is unclear whether Contact exhibits any critical feature near the transition point. On the theoretical side, it is extremely difficult to calculate exactly Contact of strongly interacting fermions near the transition temperature and certain approximations have to be made. Theoretical approaches based on different techniques lead to distinct results [10], ranging from a kink to a discontinuous jump of Contact near the transition point. Therefore, it is of fundamental importance to provide a concrete answer for the relation between Contact and phase transitions. Our approach

is to derive exact results on the behavior of Contact near a classical or quantum phase transition, based on a fundamental thermodynamic relation that is free of any approximations. These results unambiguously show that critical phenomena of Contact must exist near the transitions, and these critical phenomena are uniquely determined by the universality class of the phase transition. As our results apply to all dimensions, we use a one-dimensional exactly solvable model of strongly interacting fermions to demonstrate these critical phenomena, which shed lights on the general features of Contact near a phase transition.

We consider the fundamental thermodynamic relation,

$$dP = n d\mu + s dT + M dH - \frac{\rho_s}{2} dw^2 + c d(a_{3D}^{-1}), \quad (1)$$

where P is pressure, n , s , M , ρ_s and $c \equiv \mathcal{C}/\mathcal{V}$ are the densities of particles, entropy, magnetization, superfluid, and Contact respectively, \mathcal{V} is the volume of the system, μ , T , H and a_{3D} are the chemical potential, temperature, magnetic field and scattering length, respectively. The pre-factor $\hbar^2/(4\pi m)$ in the ordinary definition of Contact has been absorbed to c , where m is the mass. $w = v_s - v_n$ is the difference between the velocity of superfluid and normal components, which can be generated by slowly rotating the atomic cloud so that the critical velocity of the superfluid is not reached anywhere in the trap. Equation (1) has been used to measure thermodynamic quantities such as pressure and equation of state[18–21].

Here we point out that equation (1) allows one to correlate Contact with phase transitions for both classical and quantum phase transitions. First, it tells one that c must be continuous near a continuous phase transition. As c is a partial derivative of pressure, i.e., $c = (\partial P / \partial a_{3D}^{-1})_{\mu, T, H, w}$, similar to n , s , M and ρ_s , it

must be continuous based on the definition of a continuous phase transition. For instance, across the superfluid phase transition of strongly interacting fermions, c should be continuous. Second, Maxwell relations derived from equation (1) show that the derivatives of Contact with respect to μ, T, H and w exhibit critical behaviors. These Maxwell relations can be written as

$$\left(\frac{\partial c}{\partial \mu}\right)_{T,H,w,a_{3D}^{-1}} = \left(\frac{\partial n}{\partial a_{3D}^{-1}}\right)_{\mu,T,w,H}, \quad (2)$$

$$\left(\frac{\partial c}{\partial T}\right)_{\mu,H,w,a_{3D}^{-1}} = \left(\frac{\partial s}{\partial a_{3D}^{-1}}\right)_{\mu,T,w,H}, \quad (3)$$

$$\left(\frac{\partial c}{\partial H}\right)_{\mu,T,w,a_{3D}^{-1}} = \left(\frac{\partial M}{\partial a_{3D}^{-1}}\right)_{\mu,T,w,H}, \quad (4)$$

$$\left(\frac{\partial c}{\partial w^2}\right)_{\mu,T,H,a_{3D}^{-1}} = -\frac{1}{2} \left(\frac{\partial \rho_s}{\partial a_{3D}^{-1}}\right)_{\mu,T,w,H}. \quad (5)$$

Among these exact relations, equation (5) is of particular interest. It directly correlates Contact with ρ_s that characterizes superfluid phase transitions. Despite that c is finite in both normal and superfluid phases, equation (5) shows that in the normal phase, $(\partial c/\partial w^2)_{\mu,T,H,a_{3D}^{-1}} = 0$ and Contact remains unchanged after a slow rotation is turned on, since $\rho_s \equiv 0$. In the superfluid phase, ρ_s in general depends on the scattering length, and therefore $(\partial c/\partial w^2)_{\mu,T,H,a_{3D}^{-1}}$ becomes finite. In particular, in a stationary system with $w = 0$, ρ_s follows the standard scaling law near the transition point, $\rho_s = A(\delta - \delta_c(a_{3D}^{-1}))^\zeta$, where the tuning parameter $\delta = T$ and μ (or H) for classical and quantum phase transitions respectively, A is independent on δ , and ζ is the corresponding critical exponent. One then obtains the scaling law for $(\partial c/\partial w^2)_{\mu,T,H,a_{3D}^{-1}}$ near the transition point,

$$\left(\frac{\partial c}{\partial w^2}\right)_{\mu,T,H,a_{3D}^{-1}} \Big|_{w=0} = \frac{A\zeta}{2} \frac{\partial \delta_c}{\partial a_{3D}^{-1}} (\delta - \delta_c)^{\zeta-1} \quad (6)$$

Equation (6) shows the exponent of $(\partial c/\partial w^2)_{\mu,T,H,a_{3D}^{-1}}$ is entirely determined by the universality class of the superfluid phase transition. The above properties of Contact can be easily tested in experiments on trapped atoms, where superfluid and normal phases are distributed in different regions in the trap. With high resolution images available in current experiments, local Contact density c can be extracted as a function of μ using $c = (\partial P/\partial a_{3D}^{-1})_{\mu,T,H,w}$. One then could exam the distinct response of c to rotation, $(\partial c/\partial w^2)_{\mu,T,H,a_{3D}^{-1}}$, in both the superfluid and normal phases.

Equation (2,3,4) can also be implemented in experiments. Near the phase transition point, the system with $w = 0$ has the scaling law for a quantity O as $O = O_r + B_O(\delta - \delta_c(a_{3D}^{-1}))^{\eta_O}$, where $O = n, M, s, O_r$ is the regular part of O , and η_O is the corresponding critical

exponent. One then obtains

$$\left(\frac{\partial c}{\partial \mu}\right)_{T,H,w=0,a_{3D}^{-1}} = \frac{\partial n_r}{\partial a_{3D}^{-1}} - B_n \eta_n \frac{\partial \delta_c}{\partial a_{3D}^{-1}} (\delta - \delta_c)^{\eta_n-1}, \quad (7)$$

$$\left(\frac{\partial c}{\partial T}\right)_{\mu,H,w=0,a_{3D}^{-1}} = \frac{\partial s_r}{\partial a_{3D}^{-1}} - B_s \eta_s \frac{\partial \delta_c}{\partial a_{3D}^{-1}} (\delta - \delta_c)^{\eta_s-1}, \quad (8)$$

$$\left(\frac{\partial c}{\partial H}\right)_{\mu,T,w=0,a_{3D}^{-1}} = \frac{\partial M_r}{\partial a_{3D}^{-1}} - B_M \eta_M \frac{\partial \delta_c}{\partial a_{3D}^{-1}} (\delta - \delta_c)^{\eta_M-1}, \quad (9)$$

where the subscripts of the derivatives of O_r have been suppressed. The above differential forms also indicate the scaling laws of c . For instance, if one chooses $\delta = \mu$, from equation (7), one obtains $c = c_r - B_n \frac{\partial \mu_c}{\partial a_{3D}^{-1}} (\mu - \mu_c)^{\eta_n}$, where $c_r = \int_{-\infty}^{\mu} d\mu' (\partial n_r/\partial a_{3D}^{-1})$. Note that the dependences of c and n on μ have the same exponent, one concludes

$$\frac{c - c_r}{n - n_r} = -\frac{\partial \mu_c}{\partial a_{3D}^{-1}}. \quad (10)$$

In particular, if $c_r = n_r = 0$, one sees that Contact per particle in the critical region becomes a constant that is entirely determined by $-\partial \mu_c/\partial a_{3D}^{-1}$. As the non-uniform distribution of trapped atoms allows experimentalists to trace the dependence of Contact on chemical potential[18], equation (7, 10) can be directly tested in experiments.

Whereas the above discussions apply for all ultra cold atomic systems, it is useful to use an exactly solvable model to demonstrates some of these critical phenomena of Contact. Here, we consider equations (7, 10), since they can be implemented in experiments easily without a rotation. In one dimension, equation (1) becomes

$$dP = nd\mu + sdT + MdH - \frac{\rho_s}{2} dw^2 - cd(a_{1D}), \quad (11)$$

where a_{1D} is the one-dimensional scattering length and c differs from the ordinary definition by a trivial pre-factor $\hbar^2/(2m)$. Each of equations (1-10) has a direct correspondence in one dimension with a simple replacement $a_{3D}^{-1} \rightarrow -a_{1D}$. We study a one-dimensional δ -function interacting Fermi gas, described by the Yang-Gaudin Hamiltonian [22–24]

$$\mathcal{H} = -\frac{\hbar^2}{2m} \sum_{i=1}^N \frac{\partial^2}{\partial x_i^2} + g_{1D} \sum_{i=1}^{N_\uparrow} \sum_{j=1}^{N_\downarrow} \delta(x_i - x_j) + E_z \quad (12)$$

where $E_z = -\frac{1}{2}HM = -\frac{1}{2}H(n_\uparrow - n_\downarrow)$, $g_{1D} = -\frac{2\hbar^2}{ma_{1D}}$ and $a_{1D} = -a_\perp^2/a + Aa_\perp$ [25]. a_\perp is the transverse oscillation length and $A \approx 1.0326$. We introduce the polarization $P = (n_\uparrow - n_\downarrow)/n$, and define the dimensionless interaction parameter $\gamma = mg_{1D}/(n\hbar^2) = -2(na_{1D})^{-1}$ for analysis. We set the natural unit $2m = \hbar = k_B = 1$.

The model (12) has been solved using Bethe ansatz [22, 23] and has had tremendous impact in statistical

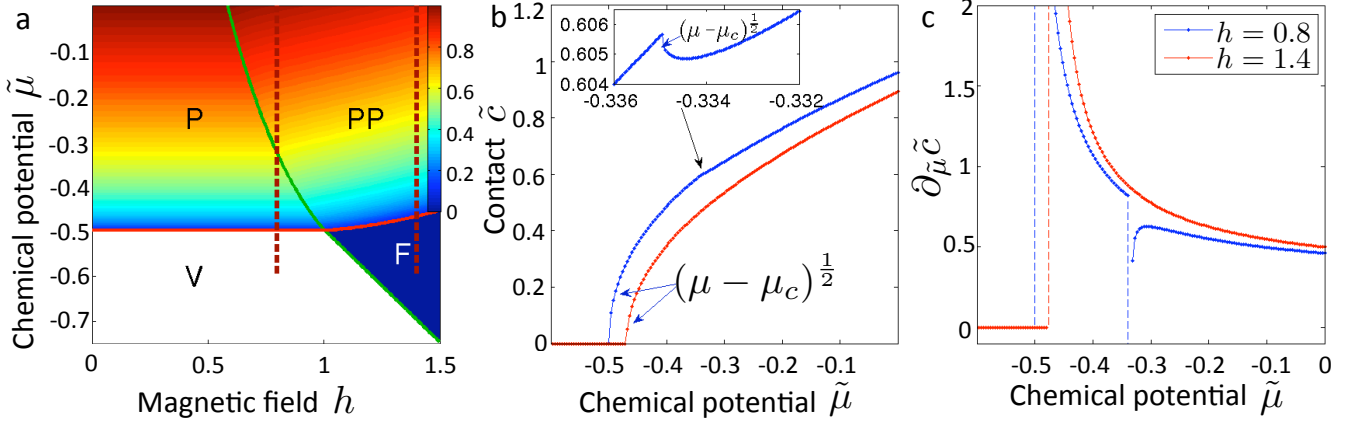


FIG. 1: Contact of one-dimensional strongly interacting fermions at zero temperature. (a) A contour plot of Contact as a function of the dimensionless chemical potential $\tilde{\mu}$ and magnetic field h . **V**, **P**, **F**, **PP** stand for vacuum, fully-paired, fully-polarised and partially-polarised phase respectively. Red and green curves represent the phase boundaries. Vertical dashed lines correspond to two cuts at fixed $h = 0.8$ and $h = 1.4$. (b) Contact is continuous across the quantum critical points. For the transition **V** – **P** and **F** – **PP**, Contact continuously increases from zero as $\tilde{c} \sim (\tilde{\mu} - \tilde{\mu}_c)^{\frac{1}{2}}$. For the transition **P** – **PP**, a kink exists as $\tilde{c} - \tilde{c}_r \sim (\tilde{\mu} - \tilde{\mu}_c)^{\frac{1}{2}}$. (c) The derivative of Contact with respect to $\tilde{\mu}$ becomes divergent as $\tilde{c} - \tilde{c}_r \sim (\tilde{\mu} - \tilde{\mu}_c)^{-\frac{1}{2}}$ in this one-dimensional system at all the transitions **V** – **P**, **P** – **PP** and **F** – **PP** for $h = 0.8$ (blue line) and $h = 1.4$ (red line).

mechanics. The experimental developments on studying one-dimensional fermions [26–30] have inspired significant interests to relate theoretical results to experimental observable [24, 31]. It was found [6, 32, 33] that, though the thermodynamic Bethe Ansatz (TBA) equations involve nontrivial collective behaviors of particles, i.e., the motion of one particle depends on all others, the summation of these complex behaviors of all individual particles leads to qualitatively new forms of simplicity in many-body phenomena [2, 35].

Contact in the extremely polarized limit with a single spin down atom and in the ground state has been studied in [37, 38]. However, reaching the goal of finding critical phenomena of Contact requires a theoretical framework capable of analytically deriving the thermodynamic properties of such gases at finite temperatures beyond mean field theory (see supplementary material). This has been a fundamental challenge in theoretical physics, due to the strong interaction between atoms. Here we compute Contact by numerically solving the TBA equations and analytically obtaining its expressions in the physical regime $T \ll \epsilon_b, H$ and $\gamma \gg 1$, and explore its critical phenomena near the phase transition. Whereas there is no finite temperature phase transition in one dimension, however there does exist universal finite temperature crossover which remarkably separates the low energy critical Tomonaga-Luttinger liquid (TLL) with relativistic dispersion from the collective matter of Free Fermi criticality with non-relativistic dispersion. Moreover, quantum phase transitions between two of the following phases, vacuum (**V**), fully-paired phase (**P**), fully-polarised phase (**F**) and partially-polarised phase

(**PP**) [2, 35] in this model provide precise description of critical phenomena of Contact in many-body systems.

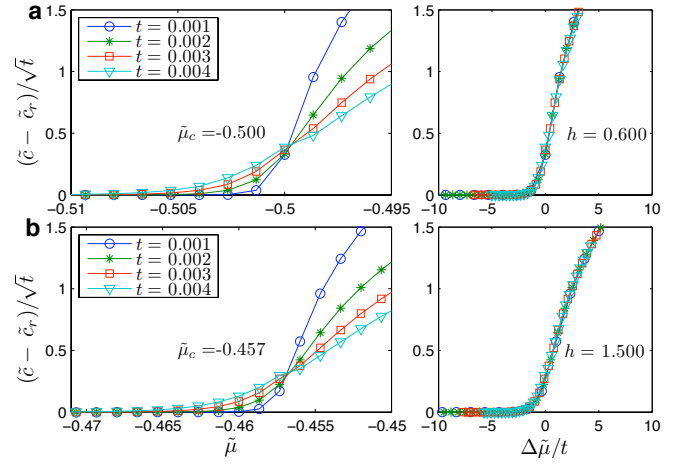


FIG. 2: Scaling laws of Contact determined by the universality class of the phase transition in the quantum critical region. The curves are obtained from the TBA equations. Left panels show the temperature-scaled Contact \tilde{c}/\sqrt{t} as a function of the chemical potential near phase boundaries **V** – **P** (a) and **F** – **PP** (b) respectively. Curves at different temperatures intersect at the quantum critical point. Right panels show that the scaled Contact vs temperature-scaled chemical potential $\Delta\tilde{\mu}/t = (\tilde{\mu} - \tilde{\mu}_c)/t$ at different temperatures collapse into a single line, a characteristic critical phenomena in the quantum critical region. These collapses confirm the dynamic exponent $z = 2$ and correlation length exponent $\nu = 1/2$.

Fig. 1 shows numerical results of the dimensionless Contact density $\tilde{c} \equiv c/\epsilon_b^2$ at zero temperature as a func-

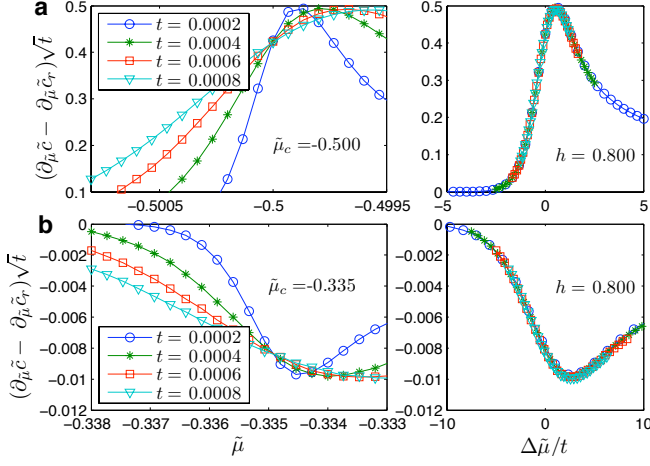


FIG. 3: Scaling laws of the derivative of Contact with respect to the chemical potential in the quantum critical region. Left panels show that different curves of $\partial\tilde{c}/\partial\tilde{\mu}$ near the transition **V** – **P** (a) and **P** – **PP** (b) intersect at the quantum critical point. Right panels show the collapse of $\partial_{\tilde{\mu}}\tilde{c}\sqrt{t}$ vs temperature-scaled chemical potential $\Delta\tilde{\mu}/t = (\tilde{\mu} - \tilde{\mu}_c)/t$ into a single curve.

tion of the dimensionless $\tilde{\mu} \equiv \mu/\epsilon_b$ and $h \equiv H/\epsilon_b$, where c is obtained from TBA equations (see supplementary material) through $c = -(\partial P/\partial a_{1D})_{\mu,H,T}$, $\epsilon_b = 2a_{1D}^{-2}$ and w has been set to be zero. Across the transition from **V** to **P**, the regular part $\tilde{c}_r \equiv 0$, since $\tilde{c} \equiv 0$ in **V**, and \tilde{c} continuously increases from zero as $\sim (\tilde{\mu} - \tilde{\mu}_c)^{1/2}$. Correspondingly, $\partial\tilde{c}/\partial\tilde{\mu}$ becomes divergent as $(\tilde{\mu} - \tilde{\mu}_c)^{-1/2}$ at this transition point. The above scaling laws of \tilde{c} and $\partial\tilde{c}/\partial\tilde{\mu}$ directly come from the scaling law of density at zero temperature near this critical point, $n \sim (\mu - \mu_c(a_{1D}))^{1/2}$. By taking the derivative of n with respect to a_{1D} , one sees that the critical exponents for \tilde{c} and $\partial\tilde{c}/\partial\tilde{\mu}$ are indeed $1/2$ and $-1/2$ respectively. Near the other transition point from **P** to **PP**, c also changes continuously with a kink $\tilde{c} - \tilde{c}_r \sim (\tilde{\mu} - \tilde{\mu}_c)^{1/2}$ and $\partial\tilde{c}/\partial\mu$ has the same $(\tilde{\mu} - \tilde{\mu}_c)^{-1/2}$ divergence.

At finite temperatures, the divergence in $\partial\tilde{c}/\partial\tilde{\mu}$ is removed. Nevertheless, critical phenomena exist for both \tilde{c} and $\partial\tilde{c}/\partial\tilde{\mu}$ in a region expanded to finite temperatures, similar to all other quantum critical phenomena. We work out the analytical expressions of \tilde{c} and derive the scaling form for \tilde{c} and its derivatives in the quantum critical region. For this regime, \tilde{c} is given explicitly by

$$\tilde{c} \approx 2\tilde{n}^b + [(\tilde{n}^b + 2\tilde{n}^u)\tilde{p}^b + 4\tilde{n}^b\tilde{p}^u], \quad (13)$$

where

$$\begin{aligned} \tilde{p}^b &= -\frac{t^{\frac{3}{2}}}{2\sqrt{\pi}}f_{\frac{3}{2}}^b(1 + \tilde{p}^b/8 + 2\tilde{p}^u), \\ \tilde{p}^u &= -\frac{t^{\frac{3}{2}}}{2\sqrt{2\pi}}f_{\frac{3}{2}}^u(1 + 2\tilde{p}^b). \end{aligned}$$

with the notation $f_{\ell}^{b,u} \equiv Li_{\ell}(-e^{\tilde{A}_{b,u}/t})$, $\tilde{A}_u = \tilde{\mu}_u - 2\tilde{p}^b -$

$\frac{t^{\frac{5}{2}}}{2\sqrt{\pi}c^3}f_{\frac{5}{2}}^b$, $\tilde{A}_b = 2\tilde{\mu}_b - \tilde{p}^b - 4\tilde{p}^u - \frac{t^{\frac{5}{2}}}{\sqrt{\pi}}\left(\frac{1}{16}f_{\frac{5}{2}}^b + \sqrt{2}f_{\frac{5}{2}}^u\right)$, and $Li_{\ell}(x) = \sum_{k=1}^{\infty} x^k/k^{\ell}$ is the polylog function. We have defined $t \equiv T/\epsilon_b$, $\tilde{n} \equiv n|a_{1D}|/2$, $\tilde{p}^{u,b} \equiv P^{u,b}|a_{1D}|/|2\epsilon_b|$, where b and u represent the quantity for bound state and unpaired particles.

It is interesting to note that upon a small correction $O(a_{1D}^3)$ the terms in the bracket of (13) is the pressure of the interacting system subtracting the one of ideal gases consisting of single fermionic atoms with the mass m and composite atoms with the mass $2m$, namely

$$\tilde{c} \approx 2\tilde{n}^b - (\tilde{p} - \tilde{p}_0), \quad (14)$$

where $\tilde{p}_0 = \tilde{p}_0^b + \tilde{p}_0^u$ with $\tilde{p}_0^b = -\frac{t^{3/2}}{2\sqrt{\pi}}Li_{3/2}(-e^{2\tilde{\mu}_b/t})$ and $\tilde{p}_0^u = -\frac{t^{3/2}}{2\sqrt{2\pi}}Li_{3/2}(-e^{\tilde{\mu}_u/t})$ (see supplementary material). This observation reveals an important nature of two-body s-wave scattering, i.e. the contact accounts for the interaction energy of fermions with different spin states. The high order corrections in the Contact (14) involve the contributions from multi-body interacting effects which are negligible in strong coupling regime. In this regard, the two-body interaction nature dominates the critical phenomena of Contact in strongly interacting Fermi gas.

Using equation (13), we find out the universal scaling form of c in the quantum critical region,

$$c = c_r + \lambda_G T^{\frac{d}{2}+1-\frac{1}{\nu z}} \mathcal{F}\left(\frac{\mu - \mu_c(a_{1D})}{T^{\frac{1}{\nu z}}}\right) \quad (15)$$

where c_r is a temperature-independent regular part, and the constant λ_G depends on μ_c , $\mathcal{F}(x)$ is a dimensionless scaling function. The dynamic and correlation length exponents have been found to be $z = 2$ and $\nu = 1/2$, see the scaling law (15) in Fig. 2. We then obtain

$$\left(\frac{\partial c}{\partial \mu}\right)_{T,H,a_{1D}} = \frac{\partial c_r}{\partial \mu} + \lambda_G T^{\frac{d}{2}+1-\frac{2}{\nu z}} \mathcal{F}'\left(\frac{\mu - \mu_c(a_{1D})}{T^{\frac{1}{\nu z}}}\right). \quad (16)$$

Fig. 3 shows the scaling behaviour of this derivative of Contact. Similar results can be obtained if one chooses H as the tuning parameter (see supplementary materials). Compare equation (15) with the standard scaling form of density in the quantum critical region, $n = n_r + \tilde{B}_n T^{\frac{d}{2}+1-\frac{1}{\nu z}} \mathcal{F}\left(\frac{\mu - \mu_c(a_{1D})}{T^{\frac{1}{\nu z}}}\right)$, we find out that $\lambda_G = \tilde{B}_n \partial\mu_c/\partial a_{1D}$ and

$$\frac{c - c_r}{n - n_r} = \frac{\partial \mu_c}{\partial a_{1D}}, \quad (17)$$

analogous to equation (10) in three dimensions. In our case, $\mu_c = -1/a_{1D}^2$ and $\partial\mu_c/\partial a_{1D} = 2/a_{1D}^3$. Equation (17) can be rewritten as $(\tilde{c} - \tilde{c}_r)/(\tilde{n} - \tilde{n}_r) = 1$. The scaling forms, equation (15-16), lead to the intersection of the scaled quantities $(c - c_r)/\sqrt{T}$ and $\sqrt{T}(\partial c/\partial \mu - \partial c_r/\partial \mu)$

for different temperatures at μ_c in our system. If one further plots these quantities as functions of $(\mu - \mu_c)/T$, different curves collapse to a single one. Such intersections and collapses are characteristic quantum critical phenomena of Contact. We have numerically confirmed the validity of these scaling forms for all interaction strengths.

We now turn to Contact per particle in the quantum critical region. To highlight the quantum critical region and other ones on the $\tilde{\mu} - t$ plane, Fig. 4 shows a density plot of entropy. The crossover temperature T^* , as shown by the white dashed line in Fig. 4, from quantum critical region to TLL region, where the density is finite for $\mu > \mu_c$ at zero temperature, is obtained from the derivation of entropy from the linear form of TLL[24]. On the other side of the transition point, the crossover temperature from the quantum critical region to the semiclassical region, where the density exponentially small, is obtained from setting thermal wave length equal to inter-particle spacing. As shown in Fig. 4 (a), if one fixes the density to be a small value, a very large portion of the trajectory of this constant density remains in the quantum critical region. As a result, \tilde{c}/\tilde{n} becomes 1. As shown in Fig. 4 (b), the numerical results of the scaled contact per particle $\tilde{c}/\tilde{n} = 1 + O(10^{-5})$ up to the temperature scale $t = 10^{-2}$, which corresponds to a ratio of the temperature to the chemical potential $t/|\tilde{\mu} - \tilde{\mu}_c| \sim 1$. These results directly confirm equation(17).

At higher densities, with increasing the temperature, the trajectory of a constant density first enters the TLL region, quickly passes the quantum critical region, and eventually enters the high temperature region with $t \gg |\tilde{\mu} - \tilde{\mu}_c|$, where entropy density becomes large and universal scaling laws of contact fail, as shown in Fig. 4 (a). Below T^* , Contact of TLL phase of the paired fermions, referred as to phase TLL_p , in the strong coupling regime is given by

$$\left(\frac{\tilde{c}}{\tilde{n}}\right)_{TLL} \approx 1 + \frac{\pi^2 \tilde{n}^3}{24} + \frac{t^2}{6\tilde{n}}. \quad (18)$$

Fig. 4 (c) shows both the numerical results of \tilde{c}/\tilde{n} at large densities and the result of the TLL theory based on equation (18). It is clear that the growth of \tilde{c}/\tilde{n} at low temperatures is described well by equation (18). The derivation from the TLL result shows a breakdown of the TLL at the crossover temperature T^* . More interestingly, one sees that before \tilde{c}/\tilde{n} eventually decreases at high temperatures, a maximum occurs around $t \approx 0.01$, which corresponds to a quantum degenerate temperature $t/(\tilde{\mu} - \tilde{\mu}_c) \sim 1 - 2$. Such a maximum indicates that Contact per particle gets enlarged in the quantum degenerate region, similar to the possible enhancement of Contact near the transition temperature of three-dimensional fermions[10].

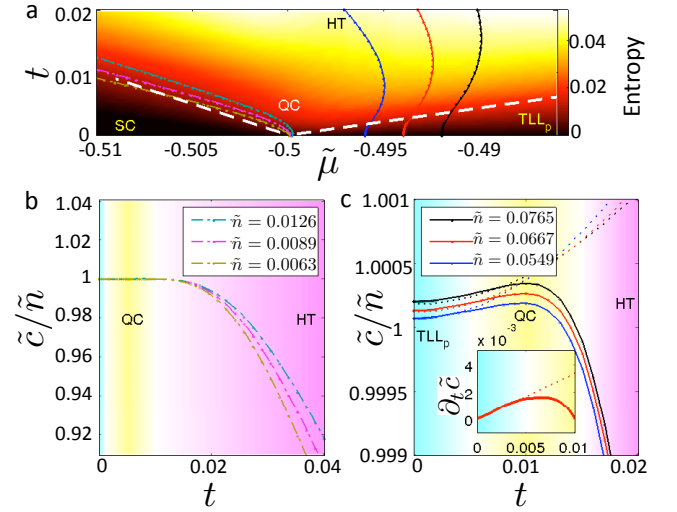


FIG. 4: Contact per particle at finite temperatures. (a): Density plot of entropy obtained from the numerical solution of the TBA equations for highlighting different regions on the $\tilde{\mu} - t$ plane. We denote SC semiclassical region with very low density. QC stand for the critical regime. TLL_p is the TLL of pairs. HT stands for high temperature region where there is no universal behaviour of thermodynamics. (b) Contact per particle \tilde{c}/\tilde{n} vs the temperature at fixed low densities. The flatness of $\tilde{c}/\tilde{n} \approx 1$ confirms the constant Contact per particle in the QC region. (c) \tilde{c}/\tilde{n} at high densities. The solid lines show the numerical result derived from the finite temperature TBA equations. The derivations of the TLL result (dotted lines) from TBA results indicate the breakdown of the TLL_p phase at the crossover temperature T^* from TLL_p to QC. T^* here is consistent with the one obtained from the derivation of entropy from the linear temperature dependence of TLL. The inset shows $\partial_t \tilde{c}$ vs temperature, in which the derivation is more visible. A maximum of \tilde{c}/\tilde{n} demonstrates the enhancement of contact when quantum effects become important in the quantum degenerate region with $t \sim \tilde{\mu} - \tilde{\mu}_c$.

Highly controllable ultra cold atoms are ideal platforms for exploring both the universality of dilute systems and the universal critical phenomena of a phase transition in many-body systems. We hope that our work will stimulate more studies on the intrinsic connection between these two types of fundamental phenomena on universality in physics.

Acknowledgments. XWG thanks R. Hulet and H.-W. Xiong for helpful discussions. This work has been supported by the National Basic Research Program of China under Grant No. 2012CB922101 and NNSFC under grant numbers 11374331 and 11304357. The work of XWG has been partially supported by the Australian Research Council. XWG thanks Chinese University of Hong Kong for kind hospitality. QZ is supported by NSFC-RGC(N-CUHK453/13) and CUHK direct grant (4053083).

* e-mail:xiwen.guan@anu.edu.au

† e-mail:qizhou@phy.cuhk.edu.hk

- [1] Tan, S., Energetics of a strongly correlated Fermi gas, *Ann. Phys.* **323**, 2952 (2008).
- [2] Tan, S., Large momentum part of a strongly correlated Fermi gas, *Ann. Phys.* **323**, 2971 (2008).
- [3] Tan, S., Generalized virial theorem and pressure relation for a strongly correlated Fermi gas, *Ann. Phys.* **323**, 2987 (2008).
- [4] Braaten, E., and Platter, L., Exact Relations for a Strongly-interacting Fermi Gas from the Operator Product Expansion, *Phys. Rev. Lett.* **100**, 205301 (2008).
- [5] Zhang, S., and Leggett, A. J., Universal properties of the ultracold Fermi gas, *Phys. Rev. A* **79**, 023601 (2009).
- [6] Werner, F., and Castin, Y., General relations for quantum gases in two and three dimensions: Two-component fermions, *Phys. Rev. A* **86**, 013626 (2012).
- [7] Werner, F., and Castin, Y., General relations for quantum gases in two and three dimensions. II. Bosons and mixtures, *Phys. Rev. A* **86**, 053633 (2012).
- [8] Stewart, J. T., Gaebler, J. P., Drake, T. E., and Jin, D. S., Verification of universal relations in a strongly interacting Fermi gas, *Phys. Rev. Lett.* **104**, 235301 (2010).
- [9] Wild, R. J., Makotyn, P., Pino, J. M., Cornell, E. A., and Jin, D. S., Measurements of Tan's contact in an atomic Bose-Einstein condensate, *Phys. Rev. Lett.* **108**, 145305 (2012).
- [10] Sagi, Y., Drake, T. E., Paudel, R., and Jin, D. S., Measurement of the Homogeneous Contact of a Unitary Fermi Gas, *Phys. Rev. Lett.* **109**, 220402 (2012).
- [11] Kuhnle, E. D., Hoinka, S., Dyke, P., Hu, H., Hannaford, P., and Vale, C. J., Temperature Dependence of the Universal Contact Parameter in a Unitary Fermi Gas, *Phys. Rev. Lett.* **106**, 170402 (2011).
- [12] Palestini, F., Perali, A., Pieri, P., and Strinati, G. C., Temperature and coupling dependence of the universal contact intensity for an ultracold Fermi gas, *Phys. Rev. A* **82**, 021605 (2010).
- [13] Enss, T., Haussmann, R., and Zwerger, W., Viscosity and scale invariance in the unitary Fermi gas, *Ann. Phys. (Paris)* **326**, 770 (2011).
- [14] Hu, H., Liu, X.-J., and Drummond P. D., Universal contact of strongly interacting fermions at finite temperatures, *New J. Phys.* **13**, 035007 (2011).
- [15] Drut, J. E., Lähde, T. A., and Ten, T., Momentum Distribution and Contact of the Unitary Fermi Gas, *Phys. Rev. Lett.* **106**, 205302 (2011).
- [16] Haussmann, R., Rantner, W., Cerrito, S., and Zwerger, W., Thermodynamics of the BCS-BEC crossover, *Phys. Rev. A* **75**, 023610 (2007).
- [17] Braaten, E., *BCS-BEC Crossover and the Unitary Fermi Gas*, Lecture Notes in Physics (Springer, 2011).
- [18] Ho, T.L., and Zhou, Q., Obtaining the phase diagram and thermodynamic quantities of bulk systems from the densities of trapped gases, *Nature Physics* **6**, 131(2010)
- [19] Nascimbène, S., Navon, N., Jiang, K. J., Chevy, F., and Salomon, C. Exploring the thermodynamics of a universal Fermi gas. *Nature* **463**, 1057 (2010)
- [20] Navon, N., Nascimbène, S., Chevy, F., and Salomon, C. The Equation of State of a Low-Temperature Fermi Gas with Tunable Interactions *Science*, **328**, 729 (2010)
- [21] Ku, M. J. H., Sommer, A. T., Cheuk, L. W., and Zwierlein, M. W., Revealing the Superfluid Lambda Transition in the Universal Thermodynamics of a Unitary Fermi Gas, *Science* **335**, 563 (2012)
- [22] Yang, C. N., Some Exact Results for the Many-Body Problem in one Dimension with Repulsive Delta-Function Interaction, *Phys. Rev. Lett.* **19**, 1312 (1967).
- [23] Gaudin, M., Un système a une dimension de fermions en interaction, *Phys. Lett. A* **24**, 55 (1967).
- [24] Guan, X.-W., Batchelor M. T., and Lee, C., Fermi gases in one dimension: From Bethe ansatz to experiments, *Rev. Mod. Phys.* **85**, 1633 (2013).
- [25] Olshanii, M., Atomic Scattering in the Presence of an External Confinement and a Gas of Impenetrable Bosons, *Phys. Rev. Lett.* **81**, 938 (1998).
- [26] Moritz, H., Stöferle, T., Günter, K., Köhl, M., and Esslinger, T., Confinement Induced Molecules in a 1D Fermi Gas, *Phys. Rev. Lett.* **94**, 210401 (2005).
- [27] Liao, Y.-A., Rittner, A. S. C., Paprotta, T., Li, W., Partridge, G. B., Hulet, R. G., Baur, S. K., and E. J. Mueller, *Nature* **467**, 567 (2010).
- [28] Zürn, G., Serwane, F., Lompe, T., Wenz, A. N., Ries, M. G., Bohn, J. E., and Jochim, S., Fermionization of Two Distinguishable Fermions, *Phys. Rev. Lett.* **108**, 075303 (2012).
- [29] Wenz, A. N., Zürn, G., Murmann, S., Brouzos, I., Lompe, T., and Jochim, S., From Few to Many: Observing the Formation of a Fermi Sea One Atom at a Time *Science* **342**, 457 (2013).
- [30] Pagano, G., Pagano, G. Mancini, M., Cappellini, G., Lombardi, P., Schäfer, F., Hu, H., i Liu, X.-J., Catani, J., Sias, C., Inguscio M., and Fallani, L., A one-dimensional liquid of fermions with tunable spin, *Nature Physics* **10**, 198 (2014).
- [31] Cazalilla, M. A., Citro, R., Giamarchi, T., Orignac, E. and Rigol, M., One dimensional bosons: From condensed matter systems to ultracold gases, *Rev. Mod. Phys.* **83**, 1405 (2011).
- [32] Takahashi, M., One-Dimensional Electron Gas with Delta-Function Interaction at Finite Temperature, *Prog. Theor. Phys.* **46**, 1388 (1971)
- [33] Yang, C. N. and Yang, C. P., Thermodynamics of a one-dimensional system of bosons with repulsive delta-function interaction, *J. Math. Phys.* **10**, 1115 (1969).
- [34] Takahashi, M., *Thermodynamics of One-Dimensional Solvable Models*, Cambridge University Press, Cambridge, (1999)
- [35] Zhao, E., Guan, X.-W., Liu, W. V., Batchelor, M. T. and Oshikawa, M., Analytic Thermodynamics and Thermometry of Gaudin-Yang Fermi Gases, *Phys. Rev. Lett.* **103**, 140404 (2009).
- [36] Guan, X.-W. and Ho, T.-L., Quantum criticality of a one-dimensional attractive Fermi gas, *Phys. Rev. A* **84**, 023616 (2011).
- [37] Doggen, E. V. H., and Kinnunen, J. J., Energy and Contact of the One-Dimensional Fermi Polaron at Zero and Finite Temperature, *Phys. Rev. Lett.* **111**, 025302 (2013)
- [38] Barth, M., and Zwerger, W., Tan relations in one dimension, *Ann. Phys.* **326**, 2544 (2011).

Supplement material

The Model

We consider the Hamiltonian of 1D spin-1/2 Fermi gas with δ -function interaction in grand canonical ensemble $\mathcal{H} = \mathcal{H}_0 - \mu N - HM$ with

$$\mathcal{H}_0 = \frac{\hbar^2}{2m} \int dx \left(\sum_{\sigma=\uparrow,\downarrow} \partial \psi_\sigma^\dagger \partial \psi_\sigma + g \psi_\uparrow^\dagger \psi_\downarrow^\dagger \psi_\downarrow \psi_\uparrow \right). \quad (19)$$

Where $N = \sum_\sigma \int dx \psi_\sigma^\dagger \psi_\sigma$ is the total particle number, $M = \frac{1}{2} \int dx (\psi_\uparrow^\dagger \psi_\uparrow - \psi_\downarrow^\dagger \psi_\downarrow)$ is the total magnization. In the above equations, μ is the chemical potential and H is the magnetic field. The interaction strength $g = -2/a_{1D}$. For $g > 0$ the interaction is repulsive and for $g < 0$ the interaction is attractive. In attractive interaction, particles with different spin form a pair with the binding energy $\epsilon_b = \frac{\hbar^2}{2m} \frac{g^2}{2}$. There are four quantum phases in the ground state: fully-polarized phase(F), fully-paired phase(P) and partially paired phase(PP) [1]. For convenience, we define the dimensionless units $\gamma = g/n$, $t = T/\epsilon_b$ and let $2m = 1$, $\hbar^2 = 1$ throughout the calculation.

For the attractive spin-1/2 Fermi gas at finite temperatures, the thermodynamics of the homogeneous system is described by two coupled Fermi gases of bound pairs and excess fermions in the charge sector and ferromagnetic spin-spin interaction in the spin sector, namely the thermodynamic Bethe ansatz (TBA) equations read [6]

$$\begin{aligned} \varepsilon^b &= 2(k^2 - \mu_b) + a_2 * \varepsilon_-^b + a_1 * \varepsilon_-^u, \\ \varepsilon^u &= k^2 - \mu_u + a_1 * \varepsilon_-^b - \sum_{m=1}^{\infty} a_m * \varepsilon_-^m, \\ \varepsilon^m &= mH + a_m * \varepsilon_-^u + \sum_{\ell=1}^{\infty} T_{m\ell} * \varepsilon_-^\ell \end{aligned} \quad (20)$$

with $m = 1, \dots, \infty$. In the above equations $*$ denotes the convolution integral, $a_m(x) = \frac{1}{2\pi} \frac{m|g|}{(mg/2)^2 + x^2}$ and $\varepsilon_-^{b,u,m} = -T \ln(1 + e^{-\varepsilon^{b,u,m}/T})$.

Here $\varepsilon^{b,u,m}$ are the dressed energies for bound pairs, excess single fermions and m -strings of spin wave bound states, respectively. These dressed energies account for excitation energies above Fermi surfaces. In the above equations the function $T_{m\ell}(k)$ is given in [3]. The effective chemical potentials of unpaired fermions and pairs were defined by $\mu_u = \mu + H/2$ and $\mu_b = \mu + \epsilon_b/2$. The thermal potential per unit length $P = p^u + p^b$ is given in terms of the effective pressures $p^{u,b} = -\frac{r}{2\pi} \int_{-\infty}^{\infty} dk \varepsilon_-^{u,b}(k)$ with $r = 1$ and 2 for the unpaired fermions and bound pairs.

The strategy for working out scaling form of Tan's contact near the critical points is to firstly perform analytical calculation of the contact near different phase transitions in the physical regime $|\gamma| \gg 1$ and $t \ll 1$. Then we

will confirm the analytical result of the universal scaling forms by numerically solving the TBA equations of the model for all interacting strength. To this end, we first present the analytical expression of the total pressure $P = p^b + p^u$ for the regime $|\gamma| \gg 1$ and $t \ll 1$ [2].

$$p^b = -\frac{1}{\sqrt{2\pi}} T^{\frac{3}{2}} Li_{\frac{3}{2}}(-e^{A_b/T}) \left(1 + \frac{p^b}{4|g|^3} + \frac{4p^u}{|g|^3}\right), \quad (21)$$

$$p^u = -\frac{1}{2\sqrt{\pi}} T^{\frac{3}{2}} Li_{\frac{3}{2}}(-e^{A_u/T}) \left(1 + \frac{4p^b}{|g|^3}\right) \quad (22)$$

with the functions

$$\begin{aligned} A_b &= 2\mu + \frac{|g|^2}{2} - \frac{p^b}{|g|} - \frac{4p^u}{|g|} - \frac{1}{4\sqrt{2\pi}|g|^3} T^{\frac{5}{2}} Li_{\frac{5}{2}}(-e^{\frac{A_b}{T}}) \\ &\quad - \frac{4}{\sqrt{\pi}|g|^3} T^{\frac{5}{2}} Li_{\frac{5}{2}}(-e^{\frac{A_u}{T}}) \end{aligned} \quad (23)$$

$$A_u = \mu + \frac{H}{2} - \frac{2p^b}{|g|} - \frac{2}{\sqrt{2\pi}|g|^3} T^{\frac{5}{2}} Li_{\frac{5}{2}}(-e^{\frac{A_b}{T}}). \quad (24)$$

In this model the $SU(2)$ spin degree of freedom ferromagnetically couples to the unpaired Fermi sea. Thus the spin wave contributions to the function A_u is negligible due to an exponentially small contributions at low temperatures, see [2]. By iteration, these effective pressures of bound pairs and unpaired fermions $p^{b,u}$ can be presented in close forms. Here a significant observation from Eq. (22) is that the pressure P can be written in term of a universal scaling form near the critical fields, i.e.

$$\tilde{P}(t, h, \tilde{\mu}) = \tilde{P}_0 + t^{d/z+1} \tilde{\mathcal{P}} \left(\frac{\tilde{\mu} - \tilde{\mu}_c}{t^{1/\nu z}}, \frac{h - h_c}{t^{1/\nu z}} \right), \quad (25)$$

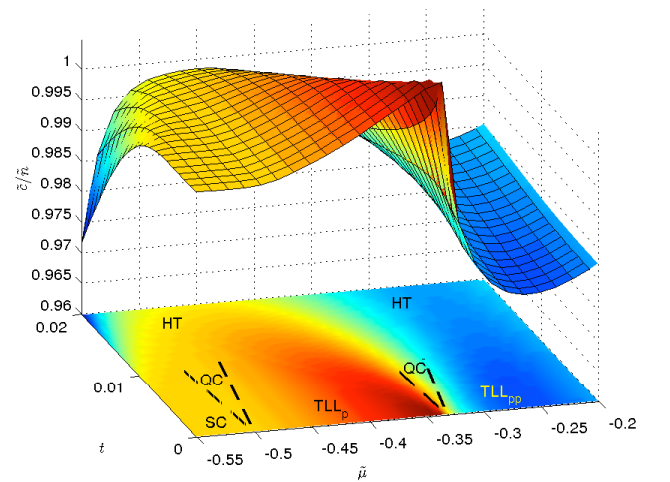


FIG. 5: 3D contour plot \tilde{c}/\tilde{n} against t and $\tilde{\mu}$ at a fixed value of $h = 0.8$. Near two critical points $\tilde{\mu}_{c1} = -0.5$ and $\tilde{\mu}_{c2} = -0.335$, different scaling behaviour are visible. See the paper about the critical phenomena of the Contact.

where the dimensionless pressure $\tilde{P} \equiv P/|g\epsilon_b|$, \tilde{P}_0 is the background pressure and $\tilde{\mathcal{P}}$ is the dimensionless scaling function. The dimensionless critical chemical potential $\tilde{\mu}_c = \mu_c/\epsilon_b$ and critical field $h_c = H_c/\epsilon_b$ depend on the interaction strength g . Therefore the Tan's contact would essentially possesses universal scaling form.

Tan's Contact

By definition of Tan's contact c

$$c = -\frac{g^2}{2} \left(\frac{\partial P}{\partial g} \right)_{\mu, H, T} \quad (26)$$

and iterating the equations (21)-(24) we obtain

$$\begin{aligned} \tilde{c} = & -\frac{1}{\sqrt{\pi}} t^{\frac{1}{2}} f_{1/2}^{A_b} - \frac{1}{2\pi} t (f_{1/2}^{A_b})^2 - \frac{1}{\sqrt{2}\pi} t f_{1/2}^{A_u} f_{1/2}^{A_b} - \frac{1}{4\pi^{3/2}} t^{\frac{3}{2}} (f_{1/2}^{A_b})^3 - \frac{5}{2\sqrt{2}\pi^{3/2}} (f_{1/2}^{A_b})^2 f_{1/2}^{A_u} - \frac{1}{8\pi^2} t^2 (f_{1/2}^{A_b})^4 \\ & - \frac{9}{4\sqrt{2}\pi^2} t^2 (f_{1/2}^{A_b})^3 f_{1/2}^{A_u} - \frac{1}{\pi^2} t^2 (f_{1/2}^{A_b})^2 (f_{1/2}^{A_u})^2 + \frac{7}{16\pi} t^2 f_{1/2}^{A_b} f_{3/2}^{A_b} + \frac{1}{\sqrt{2}\pi} t^2 f_{1/2}^{A_u} f_{3/2}^{A_b} \frac{3}{\sqrt{2}\pi} t^2 f_{1/2}^{A_b} f_{3/2}^{A_u} + O\left(t^{\frac{5}{2}}\right). \end{aligned} \quad (27)$$

Here we denote the dimensionless contact $\tilde{c} = c/\epsilon_b^2$ and $f_n^x = Li_n(-e^{x/T})$. The above equation of the contact looks very complex. Nevertheless, the universal scaling form of the contact is hidden in such complexity of this kind. In the Fig. 5 shows a 3D contour plot \tilde{c}/\tilde{n} against dimensionless temperature t and chemical potential $\tilde{\mu}$ at $h = 0.8$. Near the lower critical point $\tilde{\mu}_c = -0.5$, the flatness of \tilde{c}/\tilde{n} is the consequence of the criticality of the model as discussed in the present paper. The values of \tilde{c}/\tilde{n} drops very faster for the chemical potential excesses the upper critical point $\tilde{\mu}_c = -0.335$ due to the increase of the polarization. We will present a further discussion on the critical behaviour of the Contact.

The derivatives of the contact connect various thermal and magnetic properties such as density, magnetization and entropy

$$\frac{1}{\epsilon_b} \left(\frac{\partial c}{\partial \mu} \right)_{g, H, T} = - \left(\frac{\partial n}{\partial g} \right)_{\mu, H, T}, \quad (28)$$

$$\frac{1}{\epsilon_b} \left(\frac{\partial c}{\partial H} \right)_{g, \mu, T} = - \left(\frac{\partial m}{\partial g} \right)_{\mu, H, T}, \quad (29)$$

$$\frac{1}{\epsilon_b} \left(\frac{\partial c}{\partial T} \right)_{g, \mu, H} = - \left(\frac{\partial s}{\partial g} \right)_{\mu, H, T}. \quad (30)$$

We can analytically calculate these derivatives, namely

$$\begin{aligned} \partial_{\tilde{\mu}} \tilde{c} = & -\frac{2}{\sqrt{\pi}} t^{-\frac{1}{2}} f_{-1/2}^{A_b} - \frac{3}{\pi} f_{1/2}^{A_b} f_{-1/2}^{A_b} - \frac{2\sqrt{2}}{\pi} f_{1/2}^{A_u} f_{-1/2}^{A_b} - \frac{1}{\sqrt{2}\pi} f_{1/2}^{A_b} f_{-1/2}^{A_u} + t^{\frac{1}{2}} \left[-\frac{3}{\pi^{3/2}} (f_{1/2}^{A_b})^2 f_{-1/2}^{A_b} - \frac{9\sqrt{2}}{\pi^{3/2}} f_{1/2}^{A_b} f_{-1/2}^{A_u} f_{-1/2}^{A_b} \right. \\ & - \frac{1}{\pi^{3/2}} (f_{1/2}^{A_u})^2 f_{-1/2}^{A_b} - \frac{9}{2\sqrt{2}\pi^{3/2}} (f_{1/2}^{A_b})^2 f_{-1/2}^{A_u} \left. \right] + \frac{1}{2} t \left[-\frac{5}{\pi^2} (f_{1/2}^{A_b})^3 f_{-1/2}^{A_b} - \frac{30\sqrt{2}}{\pi^2} (f_{1/2}^{A_b})^2 f_{1/2}^{A_u} f_{-1/2}^{A_b} - \frac{27}{\pi^2} f_{1/2}^{A_b} (f_{1/2}^{A_u})^2 f_{-1/2}^{A_b} \right. \\ & - \frac{9}{2\sqrt{2}\pi^2} (f_{1/2}^{A_b})^3 f_{-1/2}^{A_u} - \frac{6\sqrt{2}}{\pi^2} (f_{1/2}^{A_b})^2 f_{-1/2}^{A_u} - \frac{6}{\pi^2} (f_{1/2}^{A_b})^2 f_{1/2}^{A_u} f_{-1/2}^{A_u} + \frac{7}{4\pi} (f_{1/2}^{A_b})^2 + \frac{5\sqrt{2}}{\pi} f_{1/2}^{A_b} f_{1/2}^{A_u} + \frac{2}{\pi} f_{-1/2}^{A_b} f_{3/2}^{A_b} \\ & \left. + \frac{\sqrt{2}}{\pi} f_{-1/2}^{A_u} f_{3/2}^{A_b} + \frac{8\sqrt{2}}{\pi} f_{-1/2}^{A_b} f_{3/2}^{A_u} \right] + O\left(t^{\frac{3}{2}}\right), \end{aligned} \quad (31)$$

$$\begin{aligned} \partial_h \tilde{c} = & -\frac{1}{\sqrt{2}\pi} f_{1/2}^{A_u} f_{-1/2}^{A_b} - \frac{1}{2\sqrt{2}\pi} f_{1/2}^{A_b} f_{-1/2}^{A_u} + \frac{1}{\sqrt{2}} t^{\frac{1}{2}} \left[-\frac{3}{2\pi^{3/2}} f_{1/2}^{A_b} f_{1/2}^{A_u} f_{-1/2}^{A_b} - \frac{1}{\sqrt{2}\pi^{3/2}} (f_{1/2}^{A_u})^2 f_{-1/2}^{A_b} - \frac{5}{4\pi^{3/2}} (f_{1/2}^{A_b})^2 f_{-1/2}^{A_u} \right] \\ & + \frac{1}{2} t \left[-\frac{3}{\sqrt{2}\pi^2} (f_{1/2}^{A_b})^2 f_{1/2}^{A_u} f_{-1/2}^{A_b} - \frac{15}{2\pi^2} f_{1/2}^{A_b} (f_{1/2}^{A_u})^2 f_{-1/2}^{A_b} - \frac{9}{4\sqrt{2}\pi^2} (f_{1/2}^{A_b})^3 f_{-1/2}^{A_u} - \frac{3}{\pi^2} (f_{1/2}^{A_b})^2 f_{1/2}^{A_u} f_{-1/2}^{A_u} \right. \\ & \left. + \frac{3}{\sqrt{2}\pi} f_{1/2}^{A_b} f_{1/2}^{A_u} + \frac{1}{\sqrt{2}\pi} f_{-1/2}^{A_u} f_{3/2}^{A_b} + \frac{\sqrt{2}}{\pi} f_{-1/2}^{A_b} f_{3/2}^{A_u} \right] + O\left(t^{\frac{3}{2}}\right). \end{aligned} \quad (32)$$

Again, we can work out the scaling functions of these

derivatives directly from the above equations. In Fig. 6,

we plot the derivative of the contact $\partial\tilde{c}/\partial\tilde{\mu}$ against chemical potential $\tilde{\mu}$. It is clearly see that the derivative of the contact evolve into a sharp peak at the critical point.

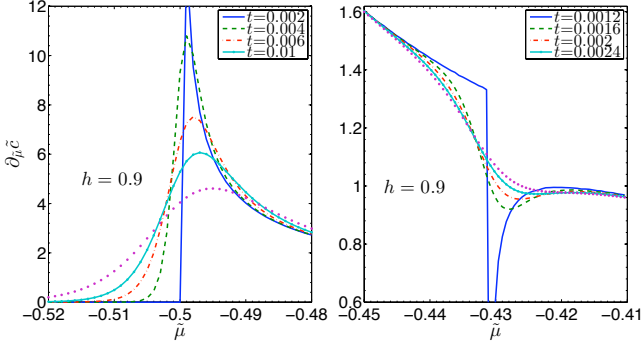


FIG. 6: Derivative of the Tan's contact with respect to chemical potential vs $\tilde{\mu}$ near the phase transitions V-P (Left panel) and P-PP (Right panel) at different temperatures. It is clearly observed that the derivative of the contact becomes divergent at $T = 0$ as the chemical potential across the two critical points. Here the critical chemical potentials $\tilde{\mu}_c = -0.5$ and $\tilde{\mu}_c = -0.431$ for V-P and P-PP phase transitions.

Universal Scaling Forms

Quantum phase transitions occur at absolute zero temperature as the driving parameters μ and H are varied across the phase boundaries. The phase transitions are driven by quantum fluctuations with quantum critical points governed by divergent correlation lengths. Near a quantum critical point, the many-body system is expected to show universal scaling behaviour in the thermodynamic quantities. In the critical regime, a universal and scale-invariant description of the system is expected through the power-law scaling of the thermodynamic properties [4, 5]. Quantum phase transitions are uniquely characterized by the critical exponents depending only on the dimensionality and symmetry of the system. In order to work out the connection of Tan's contact to the criticality of the model, we first present the dimensionless functions

$$\tilde{A}_u = A_u/\epsilon_b = \tilde{\mu} + h/2 + \frac{1}{\sqrt{\pi}} t^{\frac{3}{2}} f_{3/2}^{\tilde{A}_b}, \quad (33)$$

$$\tilde{A}_b = A_b/\epsilon_b = 2\tilde{\mu} + 1 + \frac{1}{2\sqrt{\pi}} t^{\frac{3}{2}} f_{3/2}^{\tilde{A}_b} + \frac{\sqrt{2}}{\sqrt{\pi}} t^{\frac{3}{2}} f_{3/2}^{\tilde{A}_u} \quad (34)$$

From Eqs.(33) and (34), we could expand the contact (27) in the critical regime, i.e. $|\tilde{\mu} - \tilde{\mu}_c| \ll 1$ and $|\tilde{\mu} - \tilde{\mu}_c| > t$ near different quantum phase transitions.

V-P: From vacuum V to the fully-paired phase P , the critical point is $\tilde{\mu}_c = -1/2, h < 1$. Taking low temperature limit near the critical point, we can obtain

$$\tilde{A}_u \approx (\tilde{\mu} - \tilde{\mu}_c) + (h - 1)/2, \quad \tilde{A}_b \approx 2(\tilde{\mu} - \tilde{\mu}_c), \quad (35)$$

Substituting Eq.(35) into Eq.(27), we can obtain the scaling forms of the contact and its derivative with respect to μ .

$$\begin{aligned} \tilde{c} &= -\frac{1}{\sqrt{\pi}} t^{\frac{1}{2}} Li_{\frac{1}{2}}(-e^{\frac{2(\tilde{\mu}-\tilde{\mu}_c)}{t}}), \\ \partial_{\tilde{\mu}} \tilde{c} &= -\frac{2}{\sqrt{\pi}} t^{-\frac{1}{2}} Li_{-\frac{1}{2}}(-e^{\frac{2(\tilde{\mu}-\tilde{\mu}_c)}{t}}). \end{aligned} \quad (36)$$

In this phase h_c is the constant. Therefore there does not exist scaling form of the derivative respect to H , i.e. $\partial_h \tilde{c} \approx 0$.

V-F: From the vacuum V to the fully-polarized phase F the critical point is $\tilde{\mu}_c = -h/2, h > 1$. Near the critical point, we have obtain

$$\tilde{A}_u \approx \tilde{\mu} - \tilde{\mu}_c, \quad \tilde{A}_b \approx 2(\tilde{\mu} - \tilde{\mu}_c) + 1 - h \quad (37)$$

By expansion of Eq.(27) within the critical regime, the scaling form of the Tan's contact is almost zero, i.e. $\tilde{c} = -\frac{1}{\sqrt{\pi}} t^{\frac{1}{2}} Li_{\frac{1}{2}}(-e^{\frac{1-h}{t}}) \sim 0$. This regime does not exhibit universal scaling behaviour.

F-PP: From the fully-polarized phase F to the partially-polarized phase PP , the critical point is $\tilde{\mu}_c = -1/2 + \frac{4}{3\pi}(h-1)^{3/2}$ and $h > 1$. Omitting the higher order contributions from t and $\tilde{\mu} - \tilde{\mu}_c$ we can obtain

$$\tilde{A}_u \approx (\tilde{\mu} - \tilde{\mu}_c) + a/2, \quad \tilde{A}_b \approx 2(\tilde{\mu} - \tilde{\mu}_c) \quad (38)$$

where $a = (h-1)(1 + \frac{2}{3\pi}\sqrt{h-1})$. Substituting Eq.(38) into Eq.(27), we can get the scaling forms

$$\begin{aligned} \tilde{c} &= -\frac{1}{\sqrt{\pi}} t^{\frac{1}{2}} Li_{\frac{1}{2}}(-e^{\frac{2(\tilde{\mu}-\tilde{\mu}_c)}{t}})(1 - \frac{1}{\pi} a^{1/2} + \frac{1}{\pi} a^{3/2}), \\ \partial_{\tilde{\mu}} \tilde{c} &= t^{-\frac{1}{2}} Li_{-\frac{1}{2}}(-e^{\frac{2(\tilde{\mu}-\tilde{\mu}_c)}{t}})(-\frac{2}{\sqrt{\pi}} - \frac{4}{\pi^{3/2}} a^{1/2} + \frac{2}{\pi^{5/2}} a^{3/2}). \end{aligned} \quad (39)$$

P-PP: Similar calculations can be carried out for the phase transitions from the phase P into phase PP , the critical point is $\tilde{\mu}_c = -h/2 + \frac{4}{3\pi}(1-h)^{3/2}$ and $h < 1$. Thus near the critical pint, we have

$$\tilde{A}_u \approx \tilde{\mu} - \tilde{\mu}_c, \quad \tilde{A}_b \approx 2(\tilde{\mu} - \tilde{\mu}_c) + b, \quad (41)$$

where $b = (1-h)(1 + \frac{2}{\pi}\sqrt{1-h})$. Substituting Eq.(41) into Eq.(27), we obtain the scaling forms

$$\tilde{c} = \tilde{c}_0 + t^{\frac{1}{2}} \lambda Li_{\frac{1}{2}}(-e^{\frac{\tilde{\mu}-\tilde{\mu}_c}{t}}), \quad (42)$$

$$\partial_{\tilde{\mu}} \tilde{c} = \tilde{c}_{d0} + t^{-\frac{1}{2}} \lambda_{\mu} Li_{-\frac{1}{2}}(-e^{\frac{\tilde{\mu}-\tilde{\mu}_c}{t}}). \quad (43)$$

Where the constants are given by

$$\begin{aligned} \tilde{c}_0 &= \frac{2}{\pi} b^{1/2} - \frac{2}{\pi^2} b + \frac{2}{\pi^3} b^{3/2}, \\ \lambda &= \frac{\sqrt{2}}{\pi^{3/2}} b^{1/2} - \frac{5\sqrt{2}}{\pi^{5/2}} b + \frac{9\sqrt{2}}{\pi^{7/2}} b^{3/2} - \frac{2\sqrt{2}}{3\pi^{3/2}} b^{3/2}, \\ c_{d0} &= \frac{2}{\pi} b^{-1/2} + \frac{6}{\pi^2} + \frac{12}{\pi^3} b^{1/2}, \\ \lambda_{\mu} &= \frac{\sqrt{2}}{\pi} b^{1/2} - \frac{9\sqrt{2}}{\pi^{5/2}} b. \end{aligned}$$

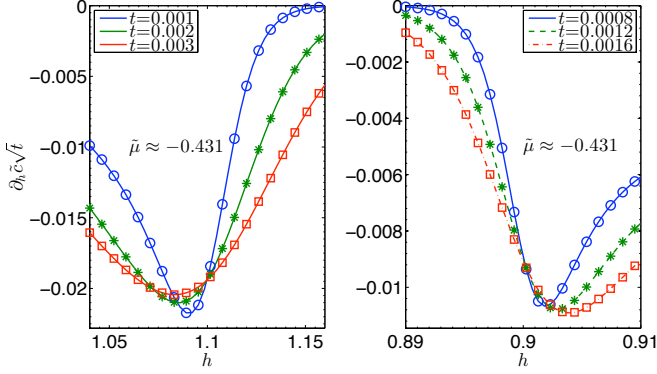


FIG. 7: Scaling behaviour of the derivative of Tan's contact $\partial_h \tilde{c} \sqrt{t}$ vs external field h . The left and (right) panel shows the intersection signature for the derivative of the contact at different temperatures near the phase transition $F - PP$ ($P - PP$). Here the critical field $h_c = 1.1$ and $h_c = 0.9$, respectively. This plot read off the critical dynamics exponent $z = 2$ and correlation length $\nu = 1/2$ respectively.

In general, at quantum criticality, the above results can be cast into the universal scaling forms

$$\tilde{c} = \tilde{c}_0 + \lambda t^{(d/z)+1-(1/\nu z)} \mathcal{F} \left(\frac{\tilde{\mu} - \tilde{\mu}_c}{t^{1/\nu z}} \right), \quad (44)$$

$$\partial_{\tilde{\mu}} \tilde{c} = \tilde{c}_{d0} + \lambda_{\mu} t^{(d/z)+1-(2/\nu z)} \mathcal{G} \left(\frac{\tilde{\mu} - \tilde{\mu}_c}{t^{1/\nu z}} \right), \quad (45)$$

where the scaling functions read off the critical dynamic exponent $z = 2$, correlation exponent $\nu = 1/2$ for contact and its derivatives. In the above equations $\tilde{c}_0, d_0, \lambda$ and λ_{μ} are constants. They are independent of the temperature. $\mathcal{F}(x), \mathcal{G}(x)$ are universal dimensionless scaling functions. Despite the analytic results were derived for the strong attractive case, the criticality is available for all interaction strength. This nature is numerically confirmed in this paper. The contact and its derivatives at different temperatures must intersect at the critical point. This feature can be used to map out the phase boundaries from the trapped gas at finite temperatures, see Fig. 7.

Moreover, we can also calculate the scaling functions for the derivative of the contact with respect to h .

F-PP: From the phase F to the phase PP, the critical point is $h_c = 1 + 2(\tilde{\mu} + h/2) \left(1 - \frac{2\sqrt{2}}{3\pi} (\tilde{\mu} + h/2)^{\frac{1}{2}} \right)$. Near the critical point we have $\tilde{A}_u \approx (h - h_c)/2 + \alpha_1$, $\tilde{A}_b \approx \beta(h - h_c)$, where $\alpha_1 = \left[\frac{3\sqrt{2}}{4} \pi (\tilde{\mu} + 1/2) \right]^{\frac{2}{3}} - \frac{16}{3\sqrt{2}\pi} (\tilde{\mu} + 1/2)^{\frac{3}{2}}$ and $\beta = \frac{1}{\sqrt{2}\pi} [3\sqrt{2}\pi (2\tilde{\mu} + 1)]^{\frac{1}{3}}$. With the help of these function, we obtain

$$\partial_h \tilde{c} = t^{-\frac{1}{2}} Li_{-\frac{1}{2}} \left(-e^{\frac{\beta(h-h_c)}{t}} \right) \left(\frac{\sqrt{2}\alpha_1^{\frac{1}{2}}}{\pi^{\frac{3}{2}}} - \frac{2\alpha_1}{\pi^{\frac{5}{2}}} - \frac{2\sqrt{2}\alpha_1^{\frac{3}{2}}}{3\pi^{\frac{3}{2}}} \right) \quad (46)$$

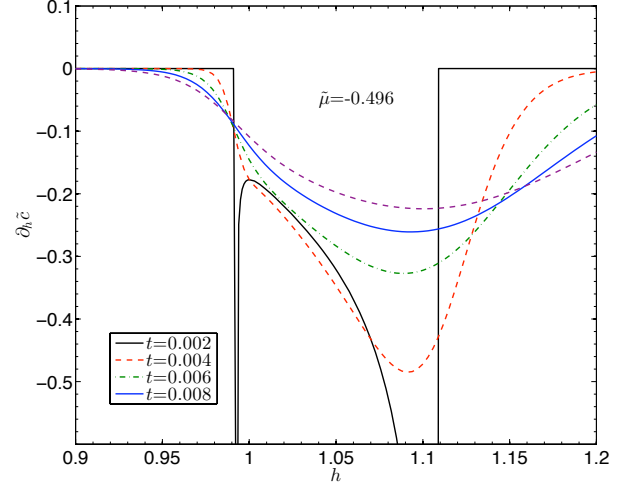


FIG. 8: The derivative of Tan's contact $\partial_h \tilde{c}$ vs h . It is clearly observed that the derivative of the contact becomes divergent at $T = 0$ as the field h varies across the two critical points. For a fixed value of $\tilde{\mu} = -0.496$ the first (second) divergent peak presents the critical behaviour of the gas for the phase transitions from P to PP and F to PP , respectively.

P-PP: From the phase P to the phase PP , the critical point is $h_c = -2\tilde{\mu} + \frac{16\sqrt{2}}{3\pi} (\tilde{\mu} + 1/2)^{\frac{3}{2}}$. Near the critical point we have $\tilde{A}_u \approx (h - h_c)/2$, $\tilde{A}_b \approx \alpha$ where $\alpha = 2\tilde{\mu} + 1 - \frac{2}{3\pi} (2\tilde{\mu} + 1)^{\frac{3}{2}}$. We obtain

$$\partial_h \tilde{c} = t^{-\frac{1}{2}} Li_{-\frac{1}{2}} \left(-e^{\frac{h-h_c}{2t}} \right) \left(\frac{1}{\sqrt{2}\pi^{\frac{3}{2}}} \alpha^{\frac{1}{2}} \right) \quad (47)$$

$$- \frac{5}{2\sqrt{2}\pi^{\frac{5}{2}}} \alpha - \frac{2\sqrt{2}}{3\pi^{\frac{3}{2}}} \alpha^{\frac{3}{2}} + \frac{9}{\sqrt{2}\pi^{\frac{7}{2}}} \alpha^{\frac{7}{2}}. \quad (48)$$

The above result of the scaling function in term of h can be also cast into the universal form

$$\partial_h \tilde{c} = \tilde{c}_{h0} + \lambda_h T^{(d/z)+1-(2/\nu z)} \mathcal{K} \left(\frac{h - h_c}{t^{1/\nu z}} \right). \quad (49)$$

Here \tilde{c}_{h0} and λ_h are constant.

NUMERICAL METHOD

In principle the TBA equations (20) in the paper present full thermodynamical properties of the model for all temperature regimes and interaction strength. Analytical result obtained above are useful to carry out full thermodynamics of the model throughout all interaction regimes. In the present paper the numerical calculations have been performed basing on the TBA equations of the spin-1/2 Fermi gas with attractive interaction (20). The TBA equations (20) involve infinite number of non-linear integral equations accounting different lengths of

spin strings (spin wave bound states). This renders one to access the thermodynamics of the model analytically and numerically. The key observation is that for n very large the function $a_n(x) \rightarrow 0$. For the string number n is greater than a critical cutoff value of the n_c -length spin strings, the value ε^{n_c} is independent of the interaction. Consequently, the contributions to the ε^u from higher spin strings, i.e. $n > n_c$, can be calculated analytically. By iteration, one finds that the value of ε^n for $n > n_c$ is the same as the solution of the TBA equations (51) with $g \rightarrow \infty$, see [6]

$$\varepsilon^n(k) := \varepsilon^{n,\infty}(k) = T \ln \left[\left(\frac{\sinh \frac{n+1}{2T} H}{\sinh \frac{H}{2T}} \right)^2 - 1 \right]. \quad (50)$$

In our numerical program, we fixed the value of n_c until the iteration error is small enough. In order to make a proper discretisation in the variable space k , we need to find a cutoff k_c for the dressed energies $\varepsilon^n(k)$ in spin sector. For $|k| \rightarrow \infty$, we see $\varepsilon^n(k) \rightarrow \varepsilon^{n,\infty}$ which is given in eq. (50), while for the charge sector $\varepsilon^{u,\infty} = \varepsilon^{b,\infty} = \infty$. Therefore for $|k| > k_c$, we use this constant dressed energy $\varepsilon^{n,\infty}$ for numerical calculation. There exists an error in comparison with the real dressed energies which is not flat in this region $|k| > k_c$. In our program, we also fix the value k_c until the iteration error is negligible.

For an arbitrary interaction strength, we are able to truncate infinite number of strings TBA equations to finite number of TBA equations in terms of the variables $\varepsilon^{b,u} = T \ln \xi^{b,u}$ and $\varepsilon^n = T \ln \eta_n$

$$\begin{aligned} \ln \xi^b(k) &= \frac{2(k^2 - c^2/4 - \mu)}{T} + a_2 * \ln(1 + \xi^b(k)^{-1}) \\ &\quad + a_1 * \ln(1 + \xi^u(k)^{-1}), \\ \ln \xi^u(k) &= S * \ln(1 + \xi^b(k)) - S * \ln(1 + \eta_1(k)), \\ \ln \eta_1(\lambda) &= S * \ln(1 + \xi^u(\lambda)^{-1}) + S * \ln(1 + \eta_2(\lambda)), \\ \ln \eta_2(\lambda) &= S * \ln(1 + \eta_3(\lambda)) + S * \ln(1 + \eta_2(\lambda)), \\ &\dots \\ \ln \eta_{n_c}(\lambda) &= 2S * \ln \left(\cosh\left(\frac{H}{2T}\right) \sqrt{1 + \eta_{n_c}(\lambda)} \right. \\ &\quad \left. + \sqrt{1 + \sinh^2\left(\frac{H}{2T}\right)(1 + \eta_{n_c}(\lambda))} \right) \\ &\quad + S * \ln(1 + \eta_{n_c-1}(\lambda)). \end{aligned} \quad (51)$$

Here the functions $S(x) = \frac{1}{2|c| \cosh(\frac{\pi x}{|g|})}$. From the parameters $\xi^b(k)$ and $\xi^u(k)$, we can get the pressures $p^{b,u}$. This new set of the TBA equations provide numerical access to the full thermodynamics of the model, including the Tomonaga-Luttinger liquid physics, quantum criticality, thermodynamics and zero temperature phase diagram.

* e-mail:xiwen.guan@anu.edu.au

† e-mail:qizhou@phy.cuhk.edu.hk

- [1] X.-W. Guan, M. T. Batchelor, C. Lee and M. Bortz, Phys. Rev. B **76**, 085120 (2007).
- [2] X.-W. Guan and T.-L. Ho, Phys. Rev. A **84**, 023616 (2011).
- [3] $T_{nm}(k) = A_{nm}(k) - \delta_{nm}\delta(k)$ with $A_{nm} = a_{|n-m|} + 2a_{(|n-m|+2)} + \dots + 2a_{(n+m-2)} + a_{(n+m)}$, see [6].
- [4] M. P. A. Fisher, P. B. Weichman, G. Grinstein and D. S. Fisher, Phys. Rev. B **40**, 546 (1989).
- [5] S. Sachdev, *Quantum Phase Transitions*, Cambridge University Press (1999).
- [6] M. Takahashi, *Thermodynamics of One-Dimensional Solvable Models*, Cambridge University Press, Cambridge, (1999).